Chinese Chemical Letters 34 (2023) 108350

Contents lists available at ScienceDirect

Chinese Chemical Letters

journal homepage: www.elsevier.com/locate/cclet

Construction of PMIA@PAN/PVDF-HFP/TiO_2 coaxial fibrous separator with enhanced mechanical strength and electrolyte affinity for lithium-ion batteries

Huilan Li, Tingting Feng*, Yufeng Liang, Mengqiang Wu*

School of Materials and Energy, University of Electronic Science and Technology of China, Chengdu 611731, China

ARTICLE INFO

Article history:
Received 12 February 2023
Revised 13 March 2023
Accepted 16 March 2023
Available online 23 March 2023

Keywords:
Poly(*m*-phthaloyl-*m*-phenylenediamine) (PMIA)
Fibrous separator
Coaxial electrospinning
Mechanical strength
Lithium-ion batteries

ABSTRACT

Poly(*m*-phthaloyl-*m*-phenylenediamine) (PMIA) is promising as the separator in lithium-ion batteries (LIBs) for its excellent thermostability, insulation and self-extinguishing properties. However, its low mechanical strength and poor electrolyte affinity limit its application in LIBs. In this work, a new PMIA@polyacrylonitrile-polyvinylidene fluoride hexafluoropropylene-titanium dioxide (PMIA@PAN/PVDF-HFP/TiO_2) composite fibrous separator with a coaxial core-shell structure was developed by combining coaxial electrospinning, hot pressing, and heat treatment techniques. This separator not only inherits the exceptional thermostability of PMIA, showing no evident thermal shrinkage at 220 °C, but also reveals improved mechanical strength (29.7 MPa) due to the formation of firm connections between fibers with the melted PVDF-HFP. Meanwhile, the massive polar groups in PVDF-HFP play a vital role in improving the electrolyte affinity, which renders the separator a high ionic conductivity of 1.36×10^{-3} S/cm. Therefore, the LIBs with PMIA@PAN/PVDF-HFP/TiO_2 separators exhibited excellent cycling and rate performance at 25 °C, and a high capacity retention rate (76.2%) at 80 °C for 200 cycles at 1 C. Besides, the lithium metal symmetric battery assembled by the separator showed a small overpotential, indicating that the separator had a role in inhibiting lithium dendrites. In short, the PMIA@PAN/PVDF-HFP/TiO_2 separator possesses a wide application prospect in the domain of LIBs.

Because of their small self-discharge, long cycle life and wide working temperature range, lithium-ion batteries (LIBs) are extensively used in various aspects of life, such as cellphones, intelligent wearable devices and electric cars [1,2]. As an indispensable component of the cell, the separator separates the anode and cathode of the cell to avoid short circuits while allowing the conduction of lithium ions. In addition, the physical and chemical properties of the separator determine the interface property and internal resistance of the cell, which has a direct influence on the electrochemical performance and safety of the battery [3,4]. Therefore, the separator with outstanding comprehensive performance is of great significance in improving the overall performance of LIBs [5]. At present, most commercial LIBs use polyolefin separators, polypropylene (PP) and polyethylene (PE). The polyolefin separators possess high mechanical strength, but exhibit low melting points, which are only 165 °C and 132 °C for PP and PE, respectively. This disadvantage would lead to a serious shrinking or even melting of the separator at high temperatures, causing safety problems. Besides, the polyolefin separator is not applicable for lithium metal batteries, because the rapid growth of lithium dendrites can easily puncture the membrane and cause short circuits [6].

To overcome the shortages of polyolefin separators, a lot of energy has been invested in new types of separators. Many methods for preparing separators have also been developed, such as non-solvent induced phase separation (NIPS) [7], *in-situ* polymerization [8], solution casting [9], electrospinning [10,11]. The nanofiber separator prepared by electrospinning has a three-dimensional network structure, large porosity, and can absorb and hold more liquid electrolytes, which is conducive to improving the ionic conductivity of the separator and the electrochemical performance of the cell [12]. Many polymers can be used for electrospinning, such as polyvinylidene fluoride (PVDF) [13], polyvinylidene fluoride hexafluoropropylene (PVDF-HFP) [14], polyacrylonitrile (PAN) [15,16], polyimide (PI) [17,18], and polymethyl methacrylate (PMMA) [19]. Among them, poly(*m*-phthaloyl-*m*-phenylenediamine) (PMIA) has attracted the attention of many researchers because of its excellent thermal stability, self-extinguishing property, and electrical insulation [20–22]. PAN is also a polymer with excellent thermal and chemical stability, and its nitrile group may interact with Li^+

* Corresponding authors.
E-mail addresses: fengtt@uestc.edu.cn (T. Feng), mwu@uestc.edu.cn (M. Wu).

https://doi.org/10.1016/j.cclet.2023.108350
1001-8417/

ions and carbonyl groups in the liquid electrolyte [23,24]. Different from PMIA and PAN, PVDF-HFP has poor thermal stability but outstanding electrolyte affinity due to the presence of fluorine, which can reduce the interface resistance and promote ion transference [25,26]. Usually, the performance of separators made of a single polymer is unsatisfactory in some aspects. Therefore, two or more polymers are often combined to obtain a composite separator with great comprehensive performance. Shuting Yang *et al*. successfully prepared a PAN@PVDF-HFP microfiber composite separator with both good electrolyte affinity and improved thermal stability by coaxial electrospinning [27]. Meanwhile, the separator showed superior cycling stability and rate performance in $LiFePO_4$/Li half cells. Bowen Cheng and his team prepared a new TBAHP (tetrabutylammonium hexafluorophosphate)/PVDF-HFP-PMIA membrane by electrospinning, which had excellent electrolyte affinity, interface compatibility, good thermal stability and super tensile strength [28]. Meanwhile, the $LiCoO_2$/Li and lithium-sulfur batteries assembled by the separator displayed excellent electrochemical performance.

Despite many advantages, the electrospinning membranes are usually poor in mechanical properties, which severely hinders their practical application in LIBs [29]. Many solutions to improve the mechanical strength of the electrospinning separators are proposed [21], such as physical or chemical crosslinking [30], hot pressing after electrospinning [31], introducing inorganic nanoparticles [32,33]. Xiaolong Leng and his team prepared a new PAN/PVDF-HFP/PVP composite separator with high porosity and outstanding mechanical strength by electrospinning, as well as a series of post-treatment methods including hot pressing, heat treatment and hydrolysis [30]. After hot pressing and heat treatment, PVDF-HFP can become an adhesive between fibers, thus increasing the tensile strength by three times (20.05 MPa); while PVP can form a porous structure as a porogen after hydrolysis. Jianhui Deng *et al*. developed a new environment-friendly cellulose/carboxylated PI (Cellulose/PI-COOH) nanofiber composite separator with high porosity and high mechanical strength by electrospinning, imidization and alkali hydrolysis [34]. Due to the three-dimensional interconnected structure generated by the cross-linked H-bond, the mechanical strength of the nanofiber composite separator was greatly improved and the tensile strength reached 34.2 MPa. Huijuan Zhao *et al*. synthesized a new type of PMIA gel polymer electrolyte doped with montmorillonite (MMT) and PVDF-HFP by electrospinning technology [25]. Relying on the strong interfacial adhesion of MMT, the surface friction between fibers was intensified, thus enhancing the mechanical property of the separator (25 MPa).

It can be seen that the mechanical properties of electrospinning membranes can be enhanced by proper modifications, and this paper intends to further enhance the mechanical strength of the electrospinning PMIA membranes and attain good electrolyte affinity by functionalizing the internal and external structures of the fibers. To this end, coaxial electrospinning, which can combine two different polymers along the axial direction and form a unique core-shell structure of fibers, is an appropriate way to prepare composite nanofiber membranes with special structures and functions. Generally, polymers with high mechanical strength and thermal stability, such as PAN, PMIA and PI, are used as the core structure, while soft materials with high electrolyte affinity, including PVDF-HFP, PVDF, and PEO, are used as the shell structure. Yue Chen *et al*. successfully prepared a PMIA@PVDF-HFP composite separator with core-shell structure *via* coaxial electrospinning technology, which displayed outstanding thermostability and mechanical properties, and the cells assembled by the separator exhibited excellent cycle stability [35]. Huijuan Zhao *et al*. prepared a new PI@F-PMIA nanofiber separator *via* coaxial electrospinning with excellent thermal stability, good interface compatibility and lithium dendrite inhibition ability [36].

In this work, we successfully prepared a composite fibrous separator with PMIA as the inner core and a mixture of PAN, PVDF-HFP and TiO_2 as the outer shell using coaxial electrospinning, followed by hot pressing and heat treatment to further improve the mechanical properties of the separator. The schematic diagram of the preparation process is shown in Fig. S1 (Supporting information). PMIA and PAN with high thermal stability were used as the dominant materials of the core and shell respectively. The introduction of PVDF-HFP in the shell can effectively improve the electrolyte affinity due to its abundant polar groups, and it can also greatly enhance the mechanical strength of the separator because PVDF-HFP can be turned as an adhesive between fibers *via* heat treatment due to its relatively low melting point (115–135 °C). Nano-TiO_2, doped as inorganic nanoparticles in the shell, is helpful to reinforce the mechanical strength of the separator and inhibit lithium dendrites. Consistent with the envisaged results, the mechanical property of the PMIA@PAN/PVDF-HFP/TiO_2 separator is greatly improved, and the tensile strength reaches 29.7 MPa, which is 1.6 times of the pure PMIA (17.6 MPa). At the same time, the PMIA@PAN/PVDF-HFP/TiO_2 separator has high porosity, great electrolyte affinity and exceptional thermal stability. Besides, the electrochemical performance of the prepared PMIA@PAN/PVDF-HFP/TiO_2 separator is also verified in $LiFePO_4$/Li half-cell which exhibits a specific discharge capacity up to 162.6 mAh/g at a current density of 0.1 C, and a capacity retention rate of 86.7% after 200 cycles at 1 C. It is worth noting that the battery could also work normally over 200 cycles at 1 C even at 80 °C. Last but not least, the Li/Li battery assembled by the separator also shows a minimum overpotential. Therefore, the PMIA@PAN/PVDF-HFP/TiO_2 separator is of great significance in developing LIBs with high safety and high-temperature application.

The SEM images of four different separators prepared by electrospinning are shown in Figs. 1a-j, where HP-170 represents the PMIA@PAN/PVDF-HFP/TiO_2 membrane after heat treatment at 170 °C, HP refers to the PMIA@PAN/PVDF-HFP/TiO_2 membrane without heat treatment, PMIA and PAN/PVDF-HFP/TiO_2 separators are prepared by the pure PMIA and PAN/PVDF-HFP/TiO_2 solution, respectively. All fibers showed smooth surfaces and were randomly arranged, forming a three-dimensional network structure. Especially, from Figs. 1b and f, it is seen that the fibers of HP-170 and PAN/PVDF-HFP/TiO_2, both of which have PVDF-HFP in the out shell, were firmly stuck to each other at the intersections due to the melted PVDF-HFP after heat treatment. However, compared with Figs. 1d and h, the fibers of HP (without heat treatment) and pure PMIA (without PVDF-HFP) separators had no such firm connections. Fig. 1i shows the magnified image of the intersection of two filaments in HP-170. Obviously, the adhesive effect of PVDF-HFP significantly improves the interaction between filaments, and thus enhancing the mechanical strength of the separators, along with the ability in inhibiting lithium dendrites. Further, to verify the core-shell structure of the HP-170 separator, the cross-section of the separator was observed. As displayed in Fig. 1j, the coaxial structure of the fibers could be expressly seen, demonstrating that the coaxial fibers were successfully prepared in the HP-170 separator. Besides, the element distributions in the fiber bundles were studied, as shown in Fig. S2 (Supporting information). It can be observed that C, N, O, F and Ti are uniformly dispersed in the fiber bundles of HP-170, which proves that PAN, PVDF-HFP and TiO_2 nanoparticles are incorporated and evenly distributed in the fiber shells of the separator.

The chemical compositions of the separators were studied by FTIR, and the spectra are exhibited in Fig. 1k. For the FTIR spectra of HP-170, HP and PAN/PVDF-HFP/TiO_2 samples, the vibration peaks at 876 cm^{-1} and 550 cm^{-1} could be assigned to the C-F and Ti-O stretching vibrations, verifying that PVDF-HFP and TiO_2 were successfully introduced into the above three composite separators

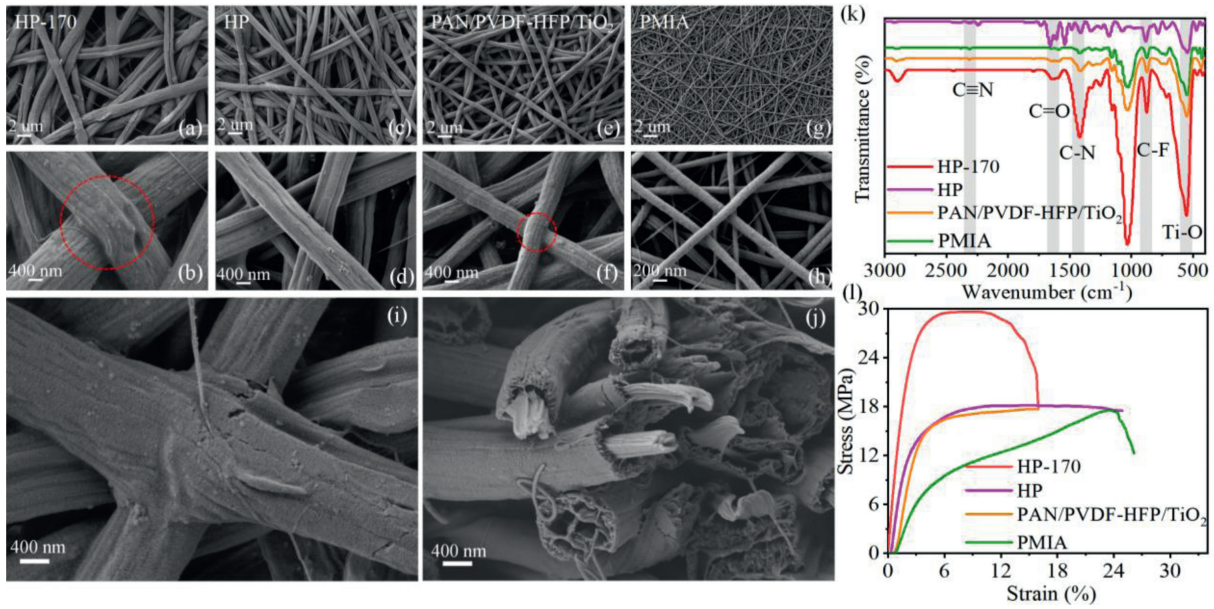

Fig. 1. (a-j) SEM images of four different electrospinning separators: (a, b) HP-170; (c, d) HP; (e, f) PAN/PVDF-HFP/TiO_2; (g, h) PMIA; (i) magnification image of HP-170; (j) cross-sectional view of HP-170. (k) FTIR spectra and (l) tensile strength of HP-170, HP, PAN/PVDF-HFP/TiO_2 and PMIA separators.

[21,37]. The characteristic peak at about 2240 cm^{-1}, attributed to the stretching vibration of C≡N, is most obvious in HP but weakened in PAN/PVDF-HFP/TiO_2, and even disappears in HP-170, which may be resulted by the oxidation of PAN when treated at 170 °C [38,39]. At the same time, the C–N stretching vibration peak of HP-170 at 1420 cm^{-1} is enhanced, which further verifies the oxidation of PAN. Moreover, the vibration peak at 1620 cm^{-1} in the spectra of PMIA, HP and HP-170 could be interpreted as the stretching vibration peak of C=O of PMIA [36].

The mechanical property of the separator, especially the tensile property, has a great impact on the safety and life of the battery [40]. Fig. 1l compares the tensile properties of the four different electrospinning separators, showing that the tensile strengths of HP-170, HP, PAN/PVDF-HFP/TiO_2 and PMIA are 29.7, 18.2, 17.7 and 17.6 MPa, respectively. The HP-170 separator has the highest tensile strength, which can be ascribed to the following three points: firstly, PVDF-HFP melts at 170 °C, and bonds the fibers as an adhesive at the intersections, thus enhancing the interfacial adhesion between fibers, as well as the tensile strength of the membrane; secondly, the PMIA core in HP-170 has high tensile strength, and can withstand high temperatures without oxidation; thirdly, the uniform distribution of nano-TiO_2 in the separator can also improve the mechanical strength of HP-170 [17,37]. Furthermore, as shown in Fig. S3 (Supporting information), the HP-170 separator could be bent, rolled and folded, and could be restored to its original appearance, which reflects the excellent flexibility of HP-170. Table S1 (Supporting information) compares the tensile strengths of HP-170 and other electrospinning membranes in previous references, which demonstrate that HP-170 has higher tensile strength and therefore is more suitable for Li-ion batteries under extreme conditions.

Thermal stability under high temperatures without shrinkage is required for the separator to ensure battery safety. In this study, the thermal shrinkage performance of the membrane was verified by treating the separators at 60 °C, 100 °C, 140 °C, 180 °C and 220 °C for 1 h, and the results are displayed in Fig. 2a. All separators had no obvious heat shrinkage below 100 °C; while Celgard 2340 obviously curled at 140 °C, and completely melted at 180 °C. Compared with Celgard 2340, the other four electrospinning separators showed excellent dimensional stability, especially

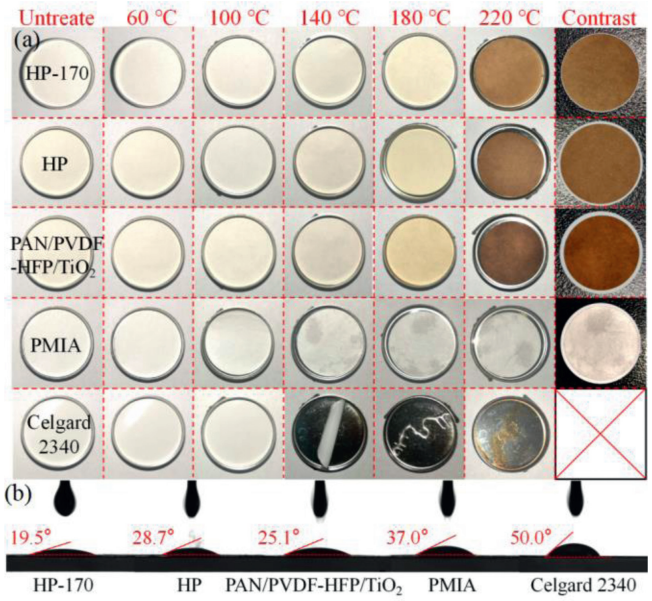

Fig. 2. (a) Thermal shrinkage tests and (b) liquid electrolyte contact angle tests of HP-170, HP, PAN/PVDF-HFP/TiO_2, PMIA and Celgard 2340 separators.

HP-170, which had almost no dimensional shrinkage after being treated at 220 °C for 1 h. It was found that the HP-170, HP and PAN/PVDF-HFP/TiO_2 membranes turned yellow and further brown, and this was resulted by the oxidation of PAN. Moreover, TG and DSC were adopted to characterize the thermostability of the membrane in Fig. S4 (Supporting information). The excellent heat resistance of HP-170 is owed to the high thermostability of PMIA and PAN, which can effectively ensure the safety of the LIBs.

Based on high mechanical strength, a high porosity and liquid electrolyte affinity are also desirable for the separator, which could provide higher electrolyte uptake, and therefore is conducive to rapid ion migration and excellent electrochemical performance of the LIBs [30]. As shown in Table S2 (Supporting information), HP-170 has the highest porosity (48.2%), higher than that of PMIA

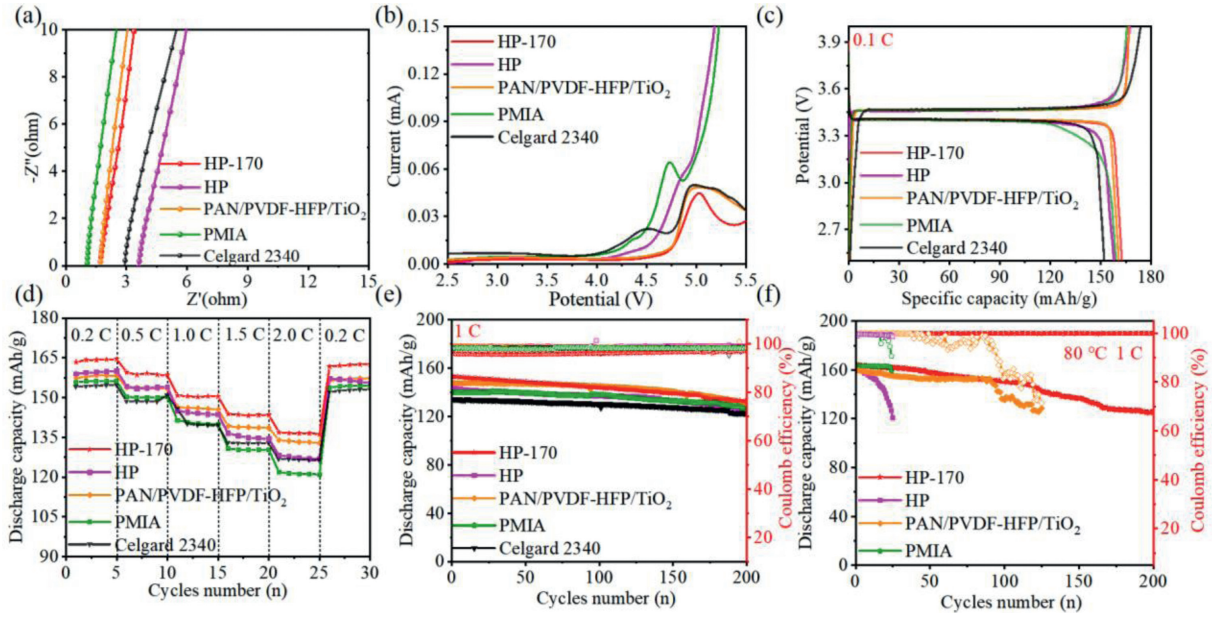

Fig. 3. (a) The electrochemical impedance spectroscopies of SS//separator//SS cells with HP-170, HP, PAN/PVDF-HFP/TiO_2, PMIA and Celgard 2340 separators. (b) Linear sweep voltammetry curves from 2.5 V to 5.5 V of the five different separators. (c) The initial charge-discharge curves at 0.1 C and (d) rate performances of the $LiFePO_4$/Li cells with HP-170, HP, PAN/PVDF-HFP/TiO_2, PMIA and Celgard 2340 separators. Cyclic stability tests of various separators (e) at room temperature and (f) at 80 °C at 1 C.

(47.7%), PAN/PVDF-HFP/TiO_2 (38.6%), HP (32.5%) and the commercial 2340 (31.1%) membranes. In addition, the liquid electrolyte wettability of the separators was investigated by static contact angles, and the results are displayed in Fig. 2b. The smaller the contact angle, the better the liquid electrolyte wettability. It is seen that the static contact angles of the commercial separator, PMIA, and HP-170 were 50.0°, 37.0° and 19.5°, respectively, indicating that the electrolyte affinity of PMIA can be effectively improved by PAN/PVDF-HFP/TiO_2 shell. Besides, the wettability of the membrane can also be directly determined by dropping 20 μL of liquid electrolyte onto the membrane and comparing the wetted area after 2 s. It could be clearly seen from Fig. S6 (Supporting information) that HP-170 had the largest wetted area, which was completely wetted, while the electrolyte on the commercial separator was still in the form of droplets, almost not absorbed by the separator. The superior wettability of HP-170 could be owed to the PAN/PVDF-HFP/TiO_2 shell with a large number of polar groups (*i.e.*, C–F, N–H, C=O, Ti–O). Particularly, PVDF-HFP has a good affinity with polar electrolytes because of the low surface energy and high polarity of the C–F bond [26]. Moreover, the polar and hydrophilic TiO_2 nanoparticles also increase the affinity for polar liquid electrolytes through Lewis acid-base binding effect [17,37]. High porosity and electrolyte affinity could usually lead to higher electrolyte adsorption. As confirmed by the experimental results (Table S2), the electrolyte uptake of HP-170 is the highest, up to 207.3%. In a word, the electrospinning HP-170 membrane with coaxial structure has a high porosity, good liquid electrolyte affinity and high electrolyte adsorption, thus providing a basis for the excellent electrochemical performance of the battery assembled with HP-170.

The ionic conductivity (σ) is a key parameter of the separator, which can be studied by AC impedance spectra of SS//separator//SS cells. As shown in Fig. 3a, the intercepts between the Nyquist curves and the x-axis represent the bulk resistances (R_0) of the separators, and the ionic conductivities of the separators were calculated according to Eq. S3 (Supporting information). As shown in Table S3 (Supporting information), HP-170 has the highest ionic conductivity (1.36×10^{-3} S/cm), much higher than that of HP (0.70×10^{-3} S/cm), PAN/PVDF-HFP/TiO_2 (0.77×10^{-3} S/cm), PMIA (0.88×10^{-3} S/cm) and Celgard 2340 (0.69×10^{-3} S/cm), which can be ascribed to its high liquid uptake and superior electrolyte wettability. At the same time, as indicated in Fig. S7 (Supporting information), the HP-170 separator has the minimum interface resistance (70 Ω) in Li//separator//Li cell, much lower than that of the commercial separator (242 Ω). Furthermore, the lithium ion transference numbers (t_{Li^+}) of Celgard 2340 and HP-170 were calculated based on Eq. S4 (Supporting information) by measuring the electrochemical impedance of the membranes before and after polarization, which is displayed in Fig. S8 (Supporting information). The t_{Li^+} of HP-170 is as high as 0.40, while that of the commercial separator is only 0.22. The high ionic conductivity, low interface impedance and high lithium ion transference number of HP-170 can also be attributed to its high electrolyte uptake and greatly enhanced electrolyte affinity introduced by the PAN/PVDF-HFP/TiO_2 shell.

The electrochemical windows of the membranes were tested by assembling Li//separator//SS batteries. Linear sweep voltammetry was performed to determine the upper limit of the electrochemical window, while cyclic voltammetry was carried out for the lower limit. It could be found from Fig. 3b that Celgard 2340 has an obvious oxidation peak at about 4.2 V, while HP-170 could maintain electrochemical stability up to 4.8 V. In Fig. S9 (Supporting information), HP-170 displays a redox peak below 0 V in the CV curve, which corresponds to the process of lithium electroplating and stripping, indicating the outstanding reduction stability of HP-170 to lithium metal. The excellent oxidation resistance and reduction stability of HP-170 indicate a large electrochemical window and potential application in high-voltage batteries.

The electrochemical properties of different separators were further studied in $LiFePO_4$//separator//Li half-cells. Fig. 3c exhibits the charge-discharge curves of the first cycle of various separators at a current density of 0.1 C. Among these separators, the battery assembled by HP-170 displays the highest initial discharge specific capacity of 162.6 mAh/g, with a coulomb efficiency of 97.44%, which can be attributed to the exceptional electrolyte affinity and the high lithium ion transference number of HP-170. The rate behaviors of various separators with a current density increasing

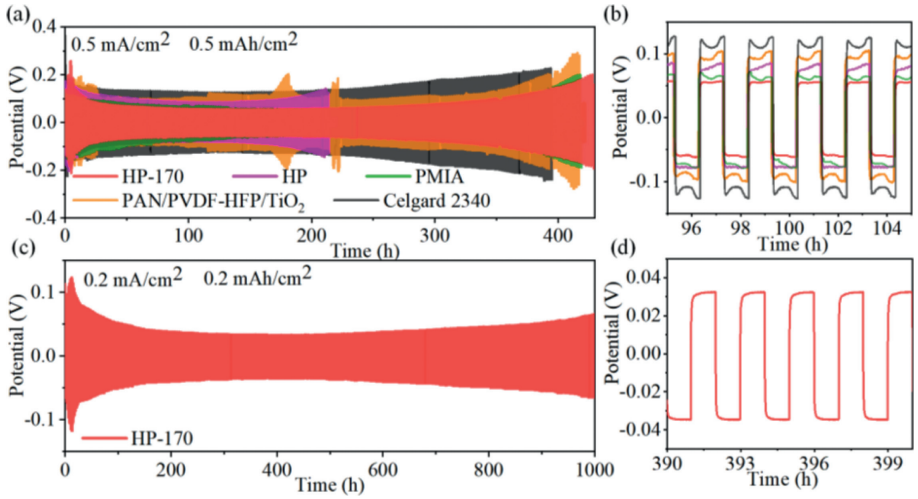

Fig. 4. (a) Voltage profiles of symmetric Li/Li cells with HP-170, HP, PAN/PVDF-HFP/TiO_2, PMIA and Celgard 2340 separators at 0.5 mA/cm^2. (b) Partial enlarged view of Fig. 4a. (c) Voltage profile of symmetric Li/Li cell with HP-170 at 0.2 mA/cm^2. (d) Partial enlarged view of Fig. 4c.

from 0.2 C to 2 C are shown in Fig. 3d. Evidently, the battery assembled with HP-170 exhibits the highest discharge specific capacities under different current densities, and the slowest capacity decay with the rising rate. Moreover, the discharge specific capacity can be fully restored when the current density returns to 0.2 C again. In contrast, the discharge specific capacity of Celgard 2340 is lower and decays rapidly. Fig. 3e compares the cycle performance of different separators at room temperature at a current density of 1 C. The HP-170 battery still displays the highest discharge specific capacity after 200 cycles, with a capacity retention rate of 86.7%, and demonstrates excellent cycle durability. The exceptional electrochemical performance of HP-170 is closely related to its great electrolyte affinity and high ionic conductivity.

In order to study the high-temperature electrochemical performance of the separators, $LiFePO_4$//separator//Li batteries were assembled and tested at 80 °C at 1 C. In Fig. 3f, the HP-170 battery shows superior high-temperature cycling stability compared with the other electrospinning membranes, exhibiting a high initial discharge specific capacity of 163.95 mAh/g, a capacity retention rate of 76.2% and a coulomb efficiency of 99.86% after 200 cycles. In contrast, the batteries with other electrospinning separators failed quickly, and the Celgard 2340 membrane was completely unable to work at high temperature. Furthermore, when compared with the counterparts reported in the previous references (Table S4 in Supporting information), HP-170 still shows excellent high-temperature performance, which can be ascribed to its excellent thermal stability. The above result confirms the application potential of the HP-170 separator in high-temperature batteries.

The lithium metal symmetrical batteries were assembled to study the lithium plating and stripping behaviors with different separators. Fig. 4a shows the lithium deposition curves at room temperature, where the current density is 0.5 mA/cm^2 and the capacity density is 0.5 mAh/cm^2. Apparently, the cell assembled by HP-170 exhibits the lowest overpotential (Fig. 4b), about 55 mV, and its time-voltage curve remains stable and smooth within 400 h, indicating that lithium dendrites are effectively suppressed. As revealed in Fig. 4c, when the current density is 0.2 mA/cm^2 and the capacity density is 0.2 mAh/cm^2, the lithium metal symmetric battery of HP-170 displays uniform lithium plating/stripping within 1000 h with a small overpotential of 30 mV (Fig. 4d). Furthermore, the rate property of HP-170 with the current density increasing from 0.5 mA/cm^2 to 2 mA/cm^2 was tested, and the result is displayed in Fig. S11 (Supporting information). It can be found that the overpotential of the Li//HP-170//Li is stable when the current density rises from 0.5 mA/cm^2 to 1.5 mA/cm^2, while the polarization rapidly intensifies at 2.0 mA/cm^2, due to a rapid and nonuniform lithium deposition at high current density. On the whole, HP-170 can inhibit lithium dendrite to a certain extent, which may be owed to the synergistic effect of the excellent interface compatibility and enhanced mechanical strength of HP-170.

In conclusion, the high-performance PMIA@PAN/PVDF-HFP/TiO_2 core-shell fibrous separator was successfully prepared by coaxial electrospinning, hot pressing and heat treatment. The introduction of the PAN/PVDF-HFP/TiO_2 shell leads to a high electrolyte affinity, which effectively enhanced the ion conductivity and greatly reduced the interface resistance. At the same time, the heat treatment of the membrane at 170 °C led to the melting of PVDF-HFP and the formation of firm bondings between fibers, hence a marked improvement in the mechanical strength of the membrane. Besides, the PMIA@PAN/PVDF-HFP/TiO_2 separator exhibited outstanding thermostability up to 220 °C and the $LiFePO_4$/Li half-battery assembled by HP-170 exhibited outstanding cycle and rate performance both at room temperature and 80 °C. Last but not least, HP-170 also showed improved performance in lithium dendrite inhibition for lithium metal batteries. Therefore, we believe that the high thermal stability, enhanced mechanical strength and good electrolyte affinity of the HP-170 separator will make it a promising separator for LIBs.

Declaration of competing interest

The authors declare that they have no known competing financial interests or personal relationships that could have appeared to influence the work reported in this paper.

Acknowledgment

This work was supported by the Natural Science Foundation of Sichuan Province (Nos. 2023YFG0096, 2022NSFSC2008 and 2023NSFSC0442).

Supplementary materials

Supplementary material associated with this article can be found, in the online version, at doi:10.1016/j.cclet.2023.108350.

References

[1] H. Lee, M. Yanilmaz, O. Toprakci, et al., Energy Environ. Sci. 7 (2014) 3857–3886.
[2] Y.J. Li, G. Zhang, B. Chen, et al., Chin. Chem. Lett. 33 (2022) 3287–3290.
[3] M.F. Lagadec, R. Zahn, V. Wood, Nat. Energy 4 (2019) 16–25.
[4] R. Xu, Y.Z. Sun, Y.F. Wang, et al., Chin. Chem. Lett. 28 (2017) 2235–2238.
[5] D.M.D. Babiker, C. Wan, B. Mansoor, et al., Compos. Part B: Eng. 211 (2021) 108658.
[6] Y.F. Yang, W.K. Wang, G.L. Meng, J.P. Zhang, J. Mater. Chem. A 10 (2022) 14137–14170.
[7] H. Zhang, C.E. Lin, M.Y. Zhou, et al., Electrochim. Acta 187 (2016) 125–133.
[8] W. Ye, J. Zhu, X.J. Liao, et al., J. Power Sources 299 (2015) 417–424.
[9] J.C. Barbosa, A. Reizabal, D.M. Correia, et al., Mater. Today Energy 18 (2020) 100494.
[10] L.Y. Yang, J.H. Cao, B.R. Cai, et al., Electrochim. Acta 382 (2021) 138346.
[11] N. Deng, Y. Wang, J. Yan, et al., J. Power Sources 362 (2017) 243–249.
[12] V.A. Agubra, L. Zuniga, D. Flores, et al., Electrochim. Acta 192 (2016) 529–550.
[13] M. Yang, Y. Ji, Y. Dong, et al., Chin. Chem. Lett. 34 (2023) 107087.
[14] T. Liang, W.H. Liang, J.H. Cao, D.Y. Wu, ACS Appl. Energy Mater. 4 (2021) 2578–2585.
[15] Y. Gao, X. Sang, Y. Chen, et al., J. Mater. Sci. 55 (2019) 3549–3560.
[16] Y. Zhai, X. Wang, Y. Chen, et al., J. Membr. Sci. 621 (2021) 118996.
[17] G. Dong, N. Dong, B. Liu, et al., J. Membr. Sci. 601 (2020) 117884.
[18] X. Gao, L. Sheng, M. Li, et al., ACS Appl. Polym. Mater. 4 (2022) 5125–5133.
[19] W.S. Khan, R. Asmatulu, V. Rodriguez, M. Ceylan, Int. J. Energy Res. 38 (2014) 2044–2051.
[20] Q. Yang, N. Deng, J. Chen, et al., Chem. Eng. J. 413 (2021) 127427.
[21] Z. Chen, Q. Lin, Y. Li, et al., Ionics (Kiel) 28 (2021) 117–125.
[22] M.C. Liu, H.J. Chen, G. Wu, et al., Chin. Chem. Lett. 34 (2023) 107546.
[23] H. Li, Z. Xu, J. Yang, et al., Sustain. Energy Fuels 4 (2020) 5469–5487.
[24] M. Guo, H. Zhu, P. Wan, et al., Adv. Fiber Mater. 4 (2022) 1511–1524.
[25] H. Zhao, W. Kang, N. Deng, et al., Chem. Eng. J. 384 (2020) 123312.
[26] H. Zhao, N. Deng, W. Kang, B. Cheng, Chem. Eng. J. 390 (2020) 124571.
[27] S. Yang, W. Ma, A. Wang, et al., RSC Adv. 8 (2018) 23390–23396.
[28] H. Zhao, N. Deng, W. Kang, et al., Energy Storage Mater. 26 (2020) 334–348.
[29] J.X. Xing, J.Y. Li, W.X. Fan, et al., Compos. Part B: Eng. 243 (2022) 110105.
[30] X.L. Leng, M.D. Yang, C.P. Li, et al., Chem. Eng. J. 433 (2022) 133773.
[31] J. Xu, L. Yuan, G. Liang, A. Gu, J. Appl. Polym. Sci. 138 (2021) 51233.
[32] N. Deng, L. Wang, Y. Feng, et al., Chem. Eng. J. 388 (2020) 124241.
[33] M. Su, Y. Chen, S. Wang, H. Wang, Chin. Chem. Lett. 34 (2023) 107553.
[34] J. Deng, D. Cao, X. Yang, G. Zhang, Chem. Eng. J. 433 (2022) 133934.
[35] Y. Chen, L.L. Qiu, X.Y. Ma, et al., Solid State Ionics 347 (2020) 115253.
[36] H. Zhao, N. Deng, G. Wang, et al., Chem. Eng. J. 404 (2021) 126542.
[37] H. Zhao, J. Yan, N. Deng, et al., J. Energy Chem. 55 (2021) 190–201.
[38] X. Zhang, S. Zhao, W. Fan, et al., Electrochim. Acta 301 (2019) 304–311.
[39] F.A. Amaral, C. Dalmolin, S.C. Canobre, et al., J. Power Sources 164 (2007) 379–385.
[40] L. Kong, Y. Wang, H. Yu, et al., ACS Appl. Mater. Interfaces 11 (2019) 2978–2988.